GLOBAL BIOGEOCHEMICAL CYCLES, VOL. 27, 1023–1033, doi:10.1002/2013GB004641, 2013

The 2008 *Emiliania huxleyi* bloom along the Patagonian Shelf: Ecology, biogeochemistry, and cellular calcification

Alex J. Poulton,[1] Stuart C. Painter,[1] Jeremy R. Young,[2] Nicholas R. Bates,[3] Bruce Bowler,[4] Dave Drapeau,[4] Emily Lyczsckowski,[4] and William M. Balch[4]

Received 30 April 2013; revised 28 August 2013; accepted 11 October 2013; published 31 October 2013.

[1] Coccolithophore blooms are significant contributors to the global production and export of calcium carbonate (calcite). The Patagonian Shelf is a site of intense annual coccolithophore blooms during austral summer. During December 2008, we made intensive measurements of the ecology, biogeochemistry, and physiology of a coccolithophore bloom. High numbers of *Emiliania huxleyi* cells and detached coccoliths ($>1 \times 10^3$ mL^{-1} and $>10 \times 10^3$ mL^{-1}, respectively), high particulate inorganic carbon concentrations (>10 mmol C m^{-2}), and high calcite production (up to 7.3 mmol C m^{-2} d^{-1}) all characterized bloom waters. The bloom was dominated by the low-calcite-containing B/C morphotype of *Emiliania huxleyi*, although a small (<10 μm) Southern Ocean diatom of the genus *Fragilariopsis* was present in almost equal numbers ($0.2–2 \times 10^3$ mL^{-1}). Estimates of *Fragilariopsis* contributions to chlorophyll, phytoplankton carbon, and primary production were >30%, similar to estimates for *E. huxleyi* and indicative of a significant role for this diatom in bloom biogeochemistry. Cell-normalized calcification rates, when corrected for a high number of nonactive cells, were relatively high and when normalized to estimates of coccolith calcite indicate excessive coccolith production in the declining phase of the bloom. We find that low measures of calcite and calcite production relative to other blooms in the global ocean indicate that the dominance of the B/C morphotype may lead to overall lower calcite production. Globally, this suggests that morphotype composition influences regional bloom inventories of carbonate production and export and that climate-induced changes in morphotype biogeography could affect the carbon cycle.

Citation: Poulton, A. J., S. C. Painter, J. R. Young, N. R. Bates, B. Bowler, D. Drapeau, E. Lyczsckowski, and W. M. Balch (2013), The 2008 *Emiliania huxleyi* bloom along the Patagonian Shelf: Ecology, biogeochemistry, and cellular calcification, *Global Biogeochem. Cycles*, *27*, 1023–1033, doi:10.1002/2013GB004641.

1. Introduction

[2] The coccolithophore *Emiliania huxleyi* frequently forms large-scale blooms in subpolar waters, where the overproduction and shedding of cellular scales (coccoliths) into the surrounding waters causes high reflectance and a milky appearance. Such blooms occur in several oceanic (e.g., Iceland Basin) and coastal (e.g., North Sea, Patagonian Shelf) regions of the world's ocean [*Brown and Yoder*, 1994; *Iglesias-Rodriguez et al*., 2002]. The Patagonian Shelf in the southwest Atlantic Ocean is one of the most prominent and largest of regular high-reflectance blooms [*Brown and Podesta*, 1997; *Garcia et al*., 2011; *Signorini et al*., 2006]. Coccolithophore blooms on the Patagonian Shelf peak in austral summer (November to January) each year [*Signorini et al*., 2006] and develop in a north to south direction [*Painter et al*., 2010]. The Patagonian Shelf is a complex hydrographic regime, where warm, low-nutrient subtropical waters from the north mix with cold, high-nutrient waters from the south [*Painter et al*., 2010]. The area also acts as a significant seasonal sink of CO_2 associated with highly productive shelf waters, with the shelf break front dominant and associated with intense biological activity [*Signorini et al*., 2006; *Schloss et al*., 2007; *Bianchi et al*., 2009].

[3] Coccolithophore blooms in the North Atlantic (e.g., Iceland Basin) are thought to be formed through a combination of high sea-surface temperatures, shallow mixed layers (<20 m), and high-irradiance conditions (>1500 μE m^{-2} s^{-1}), as well as reduced microzooplankton grazing [*Holligan et al*., 1993a; *Tyrrell and Merico*, 2004]. Blooms of *E. huxleyi* are generally believed to follow those of diatoms in waters which have become seasonally depleted in inorganic nutrients (e.g., silicic acid) and are becoming more stable in terms of vertical mixing (i.e., a seasonal thermocline) [*Holligan et al*., 1993a, 1993b]. Nitrate to phosphate ratios have been linked to bloom formation

[1]National Oceanography Centre, Southampton, UK.
[2]Department of Earth Sciences, University College London, London, UK.
[3]Bermuda Institute of Ocean Sciences, St. George's, Bermuda.
[4]Bigelow Laboratory for Ocean Sciences, East Boothbay, Maine, USA.

Corresponding author: A. J. Poulton, National Oceanography Centre, Waterfront Campus, Southampton SO14 3ZH, UK. (Alex.Poulton@noc.ac.uk)

0886-6236/13/10.1002/2013GB004641

[*Tyrrell and Merico*, 2004], although blooms often form in waters with both high and low ratios of nitrate to phosphate [*Townsend et al*., 1994; *Lessard et al*., 2005; *Painter et al*., 2010]. On the Patagonian Shelf, coccolithophore blooms have been linked with high mixed layer irradiances [*Signorini et al*., 2006; *Painter et al*., 2010; *Garcia et al*., 2011], with the bloom in 2008 in colder (<10°C) and more nutrient-rich waters (e.g., nitrate >10 μmol kg^{-1}) than found in the Iceland Basin [*Poulton et al*., 2011].

[4] As sites of intense calcite production, coccolithophore blooms are marked regions of unique biogeochemistry, where calcite production (CP) is high and organic carbon production is typically low [*Fernandez et al*., 1993; *Harlay et al*., 2011]. As *E. huxleyi* cells are relatively small (~5–6 μm), individual cells contain low amounts of chlorophyll-*a* (0.1–0.2 pg $cell^{-1}$ [*Haxo*, 1985]), and so despite high cell densities (>1000 cells mL^{-1}), coccolithophore blooms are associated with low chlorophyll-*a* (Chl) concentrations (<1–2 mg m^{-3} [*Balch et al*., 1991; *Holligan et al*., 1983, 1993a, 1993b; *Garcia et al*., 2011]). While *E. huxleyi* may dominate cell numbers, other coccolithophore species (e.g., *Coccolithus pelagicus*) and phytoplankton are often present [*Fernandez et al*., 1993; *Harlay et al*., 2011], although their net influence on bloom biogeochemistry is unclear. Coccolithophores are potentially sensitive to climate change, especially ocean acidification, whereby seawater takes up elevated atmospheric CO_2, fundamentally changing ocean pH and carbonate chemistry. Laboratory work has shown considerable intraspecies variability in *E. huxleyi* responses to changes in carbonate chemistry [*Langer et al*., 2009, 2011], and there is a need to examine natural populations along environmental gradients [e.g., *Cubillos et al*., 2007; *Beaufort et al*., 2011].

[5] In laboratory cultures, *E. huxleyi* produces and sheds excess coccoliths from its outer covering of coccoliths (coccosphere) when it experiences severe nutrient or light limitation [*Paasche*, 2002] and as growth rates slow. This continued production of coccoliths while resources limit cell division and organic production [e.g., *Müller et al*., 2008] is thought to be the main mechanism by which *E. huxleyi* forms large-scale high-reflectance blooms in the open ocean [*Balch et al*., 1996a; *Tyrrell and Merico*, 2004]. With each *E. huxleyi* cell able to produce two to three coccoliths per hour [*Paasche*, 1962; *Balch et al*., 1996b], high coccolith numbers (attached and detached) may be formed relatively rapidly, although coccolith production and detachment rates scale with rates of cellular division [*Fritz and Balch*, 1996; *Fritz*, 1999]. However, relatively few measurements of coccolith production currently exist with which to assess coccolithophore physiology in field populations.

[6] During December 2008, intensive interdisciplinary measurements were made of the hydrography, ecology, biogeochemistry, and coccolithophore physiology along the Patagonian Shelf, as part of the *Coccolithophores Of the Patagonian Shelf* (COPAS'08) expedition. Analysis of satellite images has shown that the large-scale calcite feature (Figure 1a) developed from north to south, with calcite (particulate inorganic carbon) rich waters carried north via the northward flow of the Falklands Current, and the decline of the bloom during in situ sampling was associated with an increase in sea-surface temperature [*Painter et al*., 2010]. Examination of detached coccoliths by *Poulton et al*. [2011] highlighted that *E. huxleyi* morphotype B/C (herein *E. huxleyi* B/C) dominated bloom waters and that this morphotype has a lower coccolith calcite content than other *E. huxleyi* morphotypes. The present study examines the ecological (phytoplankton community), biogeochemical (stocks and rates), and physiological (cellular calcification, coccolith production rates) characteristics of the 2008 Patagonian Shelf bloom. The two interlinked goals of the present study are to (1) assess how the characteristics of the 2008 bloom compare with other well-studied global blooms (e.g., in the Iceland Basin, Bay of Biscay) and (2) examine whether the dominance of the low coccolith-calcite *E. huxleyi* B/C affects the characteristics of the bloom.

2. Methodology

2.1. Sampling

[7] Sampling was carried out onboard the R/V *Roger Revelle* (cruise Knox22RR) which sailed from Montevideo, Uruguay (04 December 2008) to Punta Arenas, Chile (02 January 2009). The COPAS'08 cruise sampled 152 conductivity-temperature-depth (CTD) stations with 25 predawn productivity (0030 to 0800 h UT) CTD stations forming the basis of this study (Figure 1a). Depths of the mixed layer and euphotic zone were calculated following *Painter et al*. [2010] and *Poulton et al*. [2011], respectively. Water samples were collected from six light depths over the upper 100 m (55%, 33%, 14%, 7%, 5%, and 1% of near-surface irradiance) for all measurements. Light depths were determined according to *Balch et al*. [2011]. Daily downwelling irradiance, just above the sea surface ($Ed_{[0+]}$; photosynthetically active radiation (PAR)), was calculated (mol PAR m^{-2} d^{-1}) as in *Poulton et al*. [2011]. The methodology for calculating the vertical diffuse attenuation coefficient of PAR (K_d) over the water column and average mixed layer PAR irradiance ($\bar{E}d_{[ML]}$), which describes the mean light experienced by a particle mixed within the mixed layer, are outlined in *Poulton et al*. [2011].

2.2. Phytoplankton Composition

[8] At each sampling depth, coccolithophore cell numbers and species identification was performed by polarizing light microscopy following *Poulton et al*. [2010]. Coccolithophores were identified to species level under light microscopy following *Frada et al*. [2010]. For confirmation of species identification, phytoplankton counts, and analysis of *E. huxleyi* morphotypes, a separate set of surface water samples were collected for analysis by scanning electron microscopy (SEM) and analyzed as in *Poulton et al*. [2011]. Counts of phytoplankton taxa included detached coccoliths [*Poulton et al*., 2011], coccospheres, diatoms, and dinoflagellates. Coccolithophores and coccoliths were identified in SEM images following *Young et al*. [2003], while diatoms were identified following *Scott and Marchant* [2005] and *Cefarelli et al*. [2010]. Coccosphere abundances based on polarized light microscopy and SEM showed good agreement ($r = 0.955$, $p < 0.0001$, $n = 25$).

2.3. Primary Production and Calcite Production

[9] Daily rates (dawn–dawn, 24 h) of primary production (PP) and CP were determined following methodology used previously in, for example, *Poulton et al*. [2010]. Briefly, water samples from the six light depths were spiked with

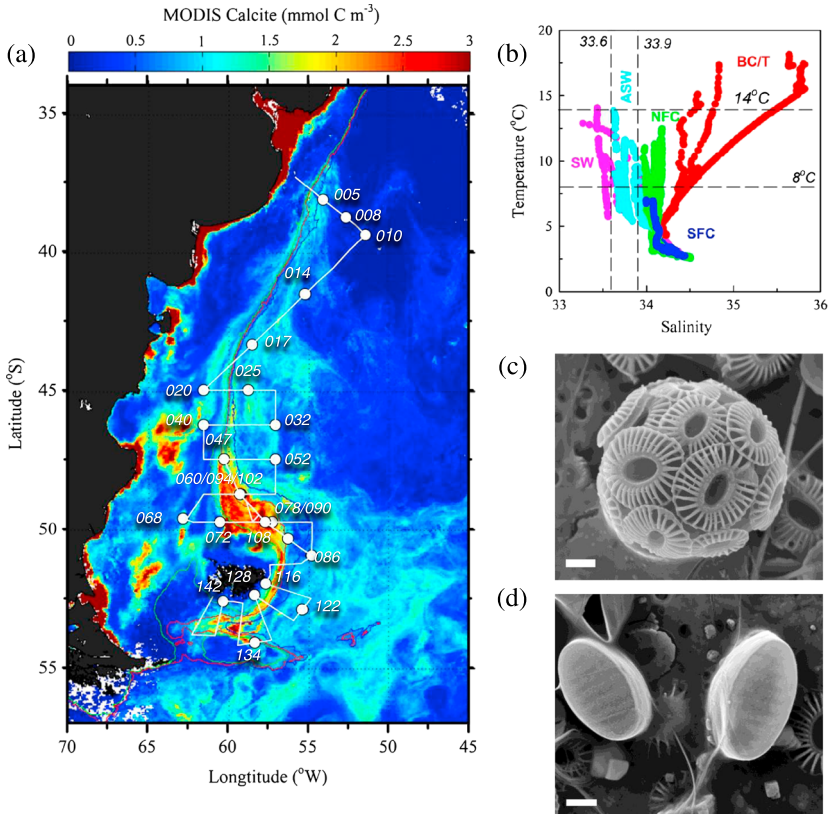

Figure 1. The 2008 Patagonian Shelf bloom. (a) Cruise track (white line) and predawn sampling stations superimposed on a December 2008 composite of surface calcite; (b) temperature versus salinity plots (full-depth CTD data) for sampling stations with hydrographic provinces separated following the analysis of *Painter et al*. [2010]; (c) scanning electron microscope (SEM) image of *Emiliania huxleyi* coccosphere showing B/C morphotype characteristics; and (d) SEM image of *Fragilariopsis* cells (likely *F. pseudonana*). Stations 060, 094, and 102 were in identical positions (Table 1). Hydrographic provinces in Figure 1b are color coded and include BC, Brazil Current; T, transitional waters; SW, shelf waters; ASW, sub-Antarctic shelf waters; NFC, Northern Falklands Current; SFC, Southern Falklands Current. White scale bars in Figures 1c and 1d are 1 µm.

60–80 µCi of ^{14}C-labeled sodium bicarbonate, including a formalin-killed blank and placed in chilled on-deck incubators with light filters (Misty blue and Grey, Lee filters^{TM}, UK) to replicate light depths. Incubations were terminated by filtration through 0.2 µm polycarbonate filters, and filters were placed in 20 mL glass vials, with organic (PP) and inorganic (CP) carbon fixation determined using the microdiffusion technique [*Paasche and Brubak*, 1994; *Balch et al*., 2000]. The microdiffusion technique separates inorganic and organic production through acidification (1 mL, 1% phosphoric acid) of the filters in gas-tight containers with a CO_2 trap (Whatman filter soaked with 200 µL ß-phenylethylamine, Sigma) which collects acid-labile production (CP), while the sample filter retains the acid-stable production (PP). Activity in both filters was determined in Ecolume^{TM} scintillation cocktail using a Beckman Coulter^{TM} LS6500 Multipurpose Scintillation Counter. Spike activity was checked in 100 µL subsamples, mixed with 100 µL of β-phenylethylamine, and Ecolume^{TM}, followed by scintillation counting. The average coefficient of variation (standard deviation/mean × 100) of triplicate PP measurements was 11% (1–54%) and 23% (1–88%) for triplicate CP measurements. On average, the formalin blank represented 25% of the CP signal (range 1–74%), with high blank contributions when rates were low at the base of the euphotic zone.

2.4. Particulate Organic Carbon, Particulate Inorganic Carbon, and Biogenic Silica

[10] Measurements of particulate organic carbon (POC) were made by filtering seawater samples (1 L) onto pre-ashed (>500°C, 12 to 18 h) Whatman GF/F filters. The filters were oven dried (50–60°C) and stored dry until acid fumed and analyzed using a Thermo Finnigan Flash EA1112 Elemental Analyzer [*Joint Global Ocean Flux Study* (*JGOFS*), 1996]. Particulate inorganic carbon (PIC) measurements were made on 0.5 L seawater samples filtered onto 0.45 µm cellulose nitrate filters, rinsed with a 0.02 mol potassium tetraborate solution, extracted in 2% nitric acid, and analyzed using inductively coupled plasma atomic optical emission spectrometry [*Poulton et al*., 2006]. Biogenic silica (BSi) measurements were made on 0.5 L seawater samples filtered onto 0.4 µm polycarbonate filters, stored at −20°C, digested in 0.2 mol sodium hydroxide, neutralized with 0.1 mol hydrochloric acid, and then analyzed using a ATI Unicam 8625 UV/VIS Spectrometer [*Brzezinski and Nelson*, 1989].

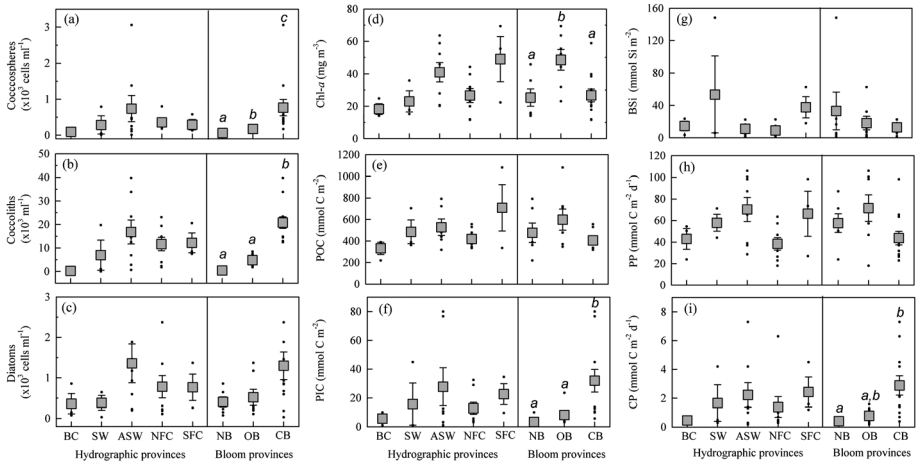

Figure 2. Average (± standard error, SE) abundances of (a) coccospheres, (b) detached coccoliths, (c) diatom cells, (d) Chl, (e) POC, (f) PIC, (g) BSi, (h) PP, and (i) CP in the different hydrographic and bloom provinces. Black dots indicate data points. Letters indicate results from pair-wise Holm-Sidak (Figure 2d) or Dunn (Figures 2a, 2b, 2f, and 2i) comparisons ($p < 0.05$).

2.5. Chlorophyll-*a*, Macronutrients, and Carbonate Chemistry

[11] Water samples (0.2 L) for Chl extraction were filtered onto Whatman GF/F filters and extracted in 10 mL 90% acetone at −20°C for 12 h [*Balch et al*., 2011]. Fluorescence was measured on a Turner Designs AU-10 fluorometer calibrated with purified chlorophyll-*a* standards. Surface macronutrient (nitrate + nitrite, phosphate, and silicic acid) concentrations were determined using an autoanalyzer following standard protocols [*Grasshoff et al*., 1983]. Samples for dissolved inorganic carbon (DIC) and total alkalinity (TA) were collected from each CTD station and opportunistically from the underway seawater supply (surface water from an intake at depth of ~5 m). Both CTD and underway surface samples were collected in ~300 mL Pyrex bottles, poisoned with $HgCL_2$, sealed, and returned to the Bermuda Institute of Ocean Sciences (BIOS) for analysis. DIC sample analyses were made using colometric methods [*Bates et al*., 1996; *Dickson et al*., 2007] and a Versatile INstrument for the Determination of Total inorganic carbon and titration Alkalinity (VINDTA) DIC system. TA sample analyses were made using potentiometric methods [*Bates et al*., 1996; *Dickson et al*., 2007] and a VINDTA TA system. Certified reference materials were routinely used for both DIC and TA analyses with the precision and accuracy of both measurements less than 0.1% or ~2 μmol kg^{-1}. Calcite saturation state (Ω_C), pH, and pCO_2 were calculated from DIC, TA, temperature, salinity, nutrient, and pressure data using the CO2Sys (CO_2 system) program [*Pierrot et al*., 2006] using the dissociation constants (p*K*'s) of *Mehrbach et al*. [1973] as refit by *Dickson and Millero* [1987]. The error associated with these calculations was typically <0.01 and <10 for pH and pCO_2, respectively.

2.6. Statistical Analysis

[12] Characteristics of the 2008 coccolithophore bloom are examined in this study using statistical comparisons of measurements within hydrographic and bloom provinces (Figures 2 and 3). Hydrographic provinces followed *Painter et al*. [2010] using a potential temperature-salinity (θ-S) diagram (Figure 1b, see section 3.1 below). Bloom provinces were based on detached coccolith abundances [*Poulton et al*., 2011]: nonbloom, $<1 \times 10^3$ coccoliths mL^{-1}; outer bloom, $1–10 \times 10^3$ coccoliths mL^{-1}; and central bloom, $>10 \times 10^3$ coccoliths mL^{-1}. For normally distributed data, one-way analysis of variance (ANOVA)

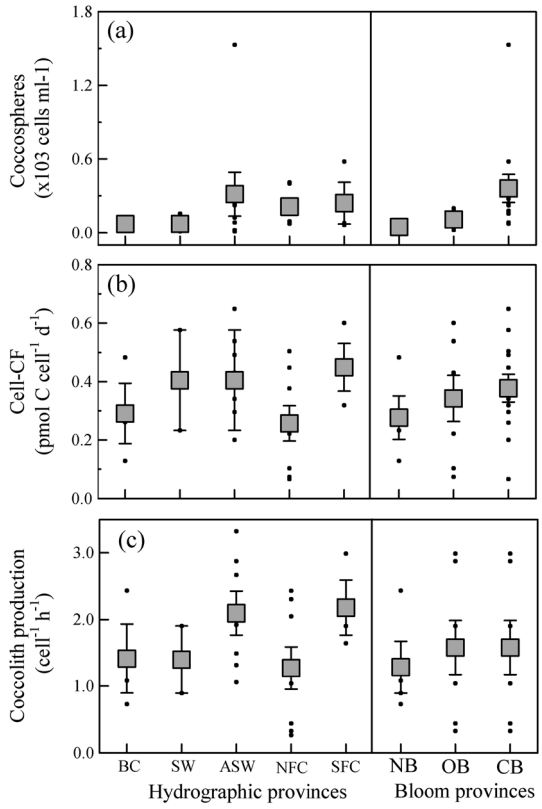

Figure 3. Average (± S.E.) values of (a) revised coccosphere abundance (see section 4.1), (b) cell-CF, and (c) coccolith production per cell in the different hydrographic and bloom provinces. Black dots indicate original data points.

Table 1. Hydrographic Characteristics of Sampling Stations Along the Patagonian Shelf [a]

Station ID	Date[b]	Latitude (°S)	Longitude (°W)	Water Depth (m)	Hydrographic Province[c]	ML (m)	Zeup (m)	SST (°C)	Salinity	Surface Macronutrients (mmol m^{-3})			$\bar{E}_{ML}$ (mol PAR m^{-2} d^{-1})	Carbonate Chemistry	
										NO_x	PO_4	dSi		pH	$\Omega_{calcite}$
005	06/12	38.07	54.03	1346	SW	9	16	18	28.7	0.1	0.24	14.2	26	8.0	3.0
008	07/12	38.46	52.38	4520	BC/T	39	63	18	35.6	0.1	0.21	1	27	8.1	5.1
010	08/12	39.23	51.24	5271	BC/T	11	40	17	34.8	1.3	0.32	2.3	36	8.2	5.6
014	09/12	41.32	55.10	5166	BC/T	25	24	15	34.6	12.4	0.43	0.6	15	8.2	4.7
017	10/12	43.22	58.27	1766	NFC	7	19	11	34.1	6.6	0.66	0.1	35	8.2	4.5
020	11/12	45.00	61.29	107	SW	7	25	14	33.4	1.1	0.45	0.1	41	8.2	5.1
025	12/12	45.00	58.43	1765	NFC	7	28	11	34.1	7.6	0.66	0.1	38	ND	ND
032	13/12	46.15	57.00	4374	NFC	21	21	12	34.2	6.9	0.67	0.5	16	8.2	4.2
040	14/12	46.15	61.29	117	ASW	19	18	14	33.6	0.4	0.46	1	8	8.2	4.5
047	15/12	47.29	60.13	603	ASW	19	24	11	33.8	7.5	0.59	0.3	20	8.2	4.7
052	16/12	47.30	57.00	4775	NFC	29	33	13	34.2	6.9	0.64	1.4	16	8.2	4.5
060	17/12	48.45	59.09	640	NFC	13	13	11	34.0	10.3	0.72	0.3	20	8.2	4.3
068	18/12	49.38	62.47	148	SW	19	35	12	33.4	6.5	0.74	0.3	28	8.1	4.0
072	19/12	49.45	60.28	171	ASW	17	27	12	33.8	1.5	0.43	0.6	22	8.3	5.0
078	20/12	49.45	57.12	353	ASW	15	26	10	33.9	12.9	0.92	0.1	16	8.1	3.7
086	21/12	50.58	54.46	1319	SFC	27	47	8	34.0	13.9	1.01	0.1	17	8.2	4.2
090	22/12	49.45	57.39	301	ASW	43	42	9	33.9	14.1	1.05	0.7	16	8.1	3.6
094	23/12	48.45	59.09	625	NFC	37	28	10	34.0	12.9	0.9	1.4	15	8.1	3.7
102	24/12	48.45	59.14	624	NFC	13	28	10	34.0	13.1	0.95	1.5	28	8.1	3.7
108	25/12	50.22	56.13	568	NFC	31	41	9	34.0	14.7	1.07	0.5	17	8.1	3.6
116	26/12	51.58	57.37	149	ASW	31	27	9	33.7	12.2	0.98	0.1	10	8.1	3.5
122	27/12	55.24	55.20	2104	SFC	59	46	7	34.1	15.6	1.17	0.1	15	8.2	3.7
128	28/12	52.23	58.19	141	ASW	61	39	9	33.7	11.8	1.05	0.5	11	8.1	3.6
134	29/12	54.06	58.18	120	SFC	60	39	7	34.0	17.1	1.33	2	6	8.1	3.3
142	30/12	52.36	60.17	185	ASW	45	34	9	33.6	10.1	0.9	0.1	8	8.2	3.8

[a]ML, mixed layer depth; Zeup, euphotic zone depth; SST, sea surface temperature; NO_x, nitrate + nitrite; PO_4, phosphate; dSi, silicic acid; $\bar{E}_{[ML]}$, average mixed layer irradiance; $\Omega_{calcite}$, calcite saturation state; ND, not determined.
[b]Dates are formatted as day/month.
[c]BC/T, Brazil current and transitional waters; SW, shelf water; ASW, Antarctic shelf water; NFC, Northern Falklands Current; SFC, Southern Falklands Current.

and pair-wise Holm-Sidak comparisons (SigmaPlot V11.0) compared differences between provinces, while for nonnormally distributed data a Kruskal-Wallis one-way ANOVA on ranks and pair-wise Dunn comparison of the ranks were used (SigmaPlot V11.0). Pearson product moment correlations (r) were performed in SigmaPlot (V11.0).

3. Results

3.1. Hydrography, Macronutrients, and Carbonate Chemistry

[13] The main trend in hydrographic conditions along the cruise track was a general decline from north to south in sea surface temperature (SST), average mixed layer irradiance ($\bar{E}_{ML}$), calcite saturation state (Ω_C) and pH, and an increase from north to south in nitrate + nitrite (NO_x) and phosphate (PO_4) concentrations (Table 1) [*Painter et al.*, 2010; *Poulton et al.*, 2011]. Salinity variations were related to inshore-offshore gradients in the different water masses present along the shelf [*Painter et al.*, 2010]. Silicic acid (dSi) and euphotic zone depth also varied, although with no obvious pattern or trend in terms of an inshore-offshore gradient or with latitude (Table 1). Concentrations of dSi were generally <2 μmol Si kg^{-1}, with only the most northerly stations (005, 010) showing concentrations >2 mol Si kg^{-1}. The total range of Ω_C and pH was 3.3 to 5.6 and 8.12 to 8.26, respectively, with Ω_C decreasing from north to south.

[14] *Painter et al.* [2010] recognized six hydrographic provinces along the Patagonian Shelf, based on a potential temperature-salinity (θ-S) diagram for water column data (Figure 1b): warm (>14°C) Brazil current (BC) and transitional waters (T) with surface salinities >34.5; shelf waters (SW) with salinities <33.6; Antarctic shelf waters (ASW) with salinities between 33.6 and 33.9; and two branches of the Falklands Current, a northern one (NFC) with warm (>8°C) surface waters and a southern one (SFC) with SSTs <8°C. Herein, we join BC and T together (BC/T) and assess the distribution of biogeochemical, ecological, and physiological properties within these hydrographic provinces. In terms of hydrographic characteristics, other than SST and salinity, the provinces are generally characterized by low macronutrients in BC/T and SW and high concentrations in NFC and SFC (Table 1).

3.2. Phytoplankton Community Composition

[15] Coccolithophore abundances in surface waters were highly variable along the Patagonian Shelf (<0.1–3.1×10^3 cells mL^{-1}) (Table 2). Detached coccolith counts also showed a large range (0–39.8×10^3 coccoliths mL^{-1}) with maximum values obviously in the central bloom (CB) (Table 2). *Emiliania huxleyi* (morphotype B/C; Figure 1c) was the common coccolithophore in waters of the Patagonian Shelf, in terms of both coccospheres and detached coccoliths [*Poulton et al.*, 2011]. The community was solely dominated by *E. huxleyi* in the outer bloom and central bloom regions, whereas a more diverse community, including species such

Table 2. Ecological and Biogeochemical Characteristics of Sampling Stations Along the Patagonian Shelf [a]

Station ID	Hydrographic Province[b]	Bloom Province[c]	Surface Water Abundance ($\times 10^3$ mL^{-1})			Euphotic Zone Integrals						
			Coccospheres (H′)	Coccoliths (H′)	Diatoms (H′)	Chl (mg m^{-2})	POC (mmol C m^{-2})	Calcite (mmol C m^{-2})	Opal (mmol Si m^{-2})	PP (mmol C m^{-2} d^{-1})	CP	CP:PP (mol:mol)
005	SW	NB	<0.1 (-)	0.0 (-)	0.5 (-)	35.9	705	1.2	148.2	58.4	0.3	0.01
008	BC	NB	0.1 (2.2)	0.4 (1.7)	0.1 (2.1)	14.1	390	6.0	23.6	23.9	0.5	0.02
010	BC	NB	0.1 (2.1)	0.2 (2.1)	0.1 (1.1)	15.9	388	10.0	16.6	50.4	0.6	0.01
014	BC	NB	0.1 (1.8)	0.2(1.6)	0.9 (0.2)	24.8	220	1.1	3.5	54.5	0.3	0.01
017	NFC	OB	0.2 (0.5)	4.0 (0.2)	0.1 (1.6)	31.9	371	4.4	7.7	18.1	0.3	0.02
020	SW	NB	0.1 (0.9)	1.1 (0.3)	0.6 (0.1)	15.2	363	1.2	5.8	71.2	0.5	0.01
025	NFC	CB	0.4 (-)	13.0 (-)	0.2 (-)	39.8	556	29.0	14.7	63.5	6.3	0.10
032	NFC	OB	0.2 (2.2)	2.3 (0.7)	0.3 (0.4)	23.1	348	3.3	1.4	46.7	0.4	0.01
040	ASW	NB	<0.1 (1.1)	0.7 (0.4)	0.2 (-)	45.9	793	1.1	1.3	87.2	0.3	<0.01
047	ASW	CB	0.5 (0.1)	23.4 (-)	1.5 (0.7)	27.9	ND	ND	ND	38.9	1.0	0.03
052	NFC	OB	0.2 (2.3)	1.8 (0.8)	0.2 (0.5)	44.3	478	3.9	7.0	57.3	0.5	0.01
060	NFC	CB	0.8(-)	14.8 (-)	0.9 (1.0)	30.4	398	5.8	1.9	40.0	0.4	0.01
068	SW	CB	0.8 (-)	19.7 (-)	0.0 (1.1)	17.8	390	44.9	6.2	44.1	4.2	0.10
072	ASW	OB	0.1 (-)	2.8 (-)	0.2 (1.4)	52.2	723	3.3	3.7	100.5	0.2	<0.01
078	ASW	CB	3.1 (-)	39.8 (-)	0.6 (1.4)	20.2	414	80.0	16.4	28.7	7.3	0.25
086	SFC	OB	0.1 (-)	7.5 (-)	1.4 (1.2)	69.4	1080	23.5	62.7	98.4	1.6	0.02
090	ASW	CB	1.4 (-)	33.9 (-)	0.9 (1.4)	20.7	319	76.7	22.5	37.0	4.2	0.11
094	NFC	CB	0.4 (-)	19.4 (-)	0.8 (0.4)	11.9	335	13.8	11.2	22.9	1.0	0.04
102	NFC	CB	0.3 (-)	14.8 (-)	1.3 (0.2)	11.6	338	10.0	5.7	26.5	1.5	0.06
108	NFC	CB	0.4 (0.1)	23.1 (-)	2.4 (0.6)	20	531	32.5	22.7	31.9	0.7	0.02
116	ASW	CB	0.5 (-)	14.5 (-)	1.9 (1.1)	58.9	ND	12.7	10.0	98.3	2.1	0.02
122	SFC	OB	0.2 (0.1)	8.5 (-)	0.3 (1.6)	55.4	710	9.7	32.3	73.5	1.2	0.02
128	ASW	CB	0.2 (0.1)	12.5 (-)	4.4 (0.8)	38.5	440	10.7	11.9	65.4	1.4	0.02
134	SFC	CB	0.6 (0.1)	20.6 (-)	0.7 (1.5)	22.4	336	34.6	18.1	27.0	4.5	0.17
142	ASW	OB	0.3 (0.1)	6.9 (-)	1.2 (0.9)	63.6	480	9.3	12.4	106	1.3	0.01

[a]H′, Shannon-Weiner diversity; Chl, Chlorophyll-*a*; POC, particulate organic carbon; PP, primary production; CP, calcite production, ND, not determined.
[b]BC/T, Brazil current and transitional waters; SW, shelf water; ASW, Antarctic shelf water; NFC, Northern Falklands Current; SFC, Southern Falklands Current.
[c]NB, nonbloom; OB, outer bloom; CB, central bloom.

as *Syracosphaera delicata*, *Umbellosphaera tenuis*, and *Syracosphaera marginaporata*, were found in the nonbloom region [*Poulton et al*., 2011]. This is reflected by high values (>1.8) of the Shannon-Weiner diversity index for coccospheres and detached coccoliths in association with the nonbloom region (Table 2). Coccosphere and detached coccolith abundances showed patterns with hydrographic province (Figures 2a and 2b), with average abundances higher in ASW, although no significant difference was detected (one-way ANOVA, $p > 0.2$). Significant differences (one-way ANOVA on rank abundances, $p < 0.001$) for both coccospheres and coccoliths occurred between bloom provinces, with central bloom coccosphere and coccolith abundances significantly ($p < 0.05$) higher than in other provinces (Figures 2a and 2b).

[16] Diatoms were also abundant along the shelf, ranging in abundance from 0.1 to 4.4×10^3 cells mL^{-1} (Table 2), with diatom counts higher than coccosphere counts at stations at both ends of the gradient in coccolithophore density. The diatom community was represented by a much more diverse group of species, as reflected in the moderately high (>1.0) values of Shannon-Weiner diversity, and these were found at stations associated with all bloom provinces (Table 2). Diatoms along the shelf included several species from the genera *Chaetoceros*, *Thalassiosira*, and *Pseudonitzschia*, although a small (<10 µm) *Fragilariopsis* species (likely *Fragilariopsis pseudonana* [*Cefarelli et al*., 2010]) dominated numerically (Figure 1d; 0.02–2.0×10^3 cells mL^{-1}) at many of the sampling stations. Average diatom abundances were higher in ASW and the central bloom region (Figure 2c), although no significant differences (one-way ANOVA, $p > 0.1$) were found.

3.3. Chlorophyll-*a* and Particulate Material (POC, Calcite, and Opal)

[17] Euphotic zone integrals of Chl varied from 11.6 to 69.4 mg m^{-2}, with high (and low) values associated with both the central bloom and nonbloom regions, respectively (Table 2). No significant differences were found in terms of Chl between hydrographic provinces (one-way ANOVA, $p > 0.05$), whereas a significant difference was found between bloom provinces (one-way ANOVA, $p < 0.01$), with concentrations significantly higher in the outer bloom region (Figure 2d). Euphotic zone POC varied from 220 to 1080 mmol C m^{-2} along the shelf, showing a similar pattern to Chl ($r = 0.771$, $p < 0.001$, $n = 23$). However, no significant differences were observed in terms of POC within hydrographic or bloom provinces (Figure 2e).

[18] Particulate inorganic carbon (PIC) concentrations ranged from 1.1 to 80 mmol C m^{-2} (Table 2), showing no correlation with Chl or POC ($p > 0.2$), or significant differences between hydrographic provinces (Figure 2f). As expected, however, PIC concentrations were significantly different between bloom provinces (one-way ANOVA, $p < 0.001$), with concentrations significantly higher in the central bloom (Figure 2f). Ratios of PIC to POC (mol:mol) ranged from 0.001 to 0.241, with higher ratios associated with outer bloom and central bloom regions (data not shown). Biogenic silica (BSi) concentrations ranged from 1.3 to 148.2 mmol m^{-2}, with higher concentrations often

Table 3. Average (Range) Percentage Contributions From *Emiliania huxleyi* and *Fragilariopsis* to Carbon, Chlorophyll, and Primary Production[a]

Region	*Emiliania huxleyi*			Inactive Cells (% Total)[d]	*Fragilariopsis*		
	PhytoC[b]	Chl[b]	PP[c]		PhytoC[e]	Chl[e]	PP[f]
				Hydrographic provinces			
BC/T	5	6	4	0	4	4	2
	(2–8)	(2–9)	(1–7)		(0.1–10)	(0.1–9)	(0.1–6)
SW	4	5	5	30	3	3	3
	(0.1–12)	(0.1–13)	(1–13)	(0–80)	(0.1–9)	(0.1–8)	(0.1–7)
ASW	7	8	8	30	3	4	3
	(0.1–34)	(0.1–38)	(0.1–34)	(0–70)	(0.2–7)	(0.3–12)	(0.3–11)
NFC	4	4	3	40	11	13	12
	(1–8)	(2–9)	(1–8)	(0–80)	(0.3–35)	(0.3–41)	(0.3–39)
SFC	7	8	9	80	2	3	3
	(1–18)	(1–20)	(2–23)	(0–50)	(0.1–4)	(0.2–6)	(0.2–6)
				Bloom province			
NB	3	3	2	0	3	4	3
	(0.1–8)	(0.1–9)	(0.1–7)		(0.1–7)	(0.1–10)	(0.1–9)
OB	2	2	2	10	1	1	1
	(1–4)	(1–4)	(0.1–2)	(0–50)	(0.1–2)	(0.2–3)	(0.2–3)
CB	9	10	10	50	9	11	11
	(1–34)	(2–38)	(1–34)	(0–80)	(0.4–35)	(0.3–41)	(0.3–39)

[a]PhytoC, phytoplankton carbon; Chl, chlorophyll-*a;* PP, primary production.
[b]Estimated from cell counts using 0.6 pmol C cell^{-1} and 0.2 pg Chl cell^{-1} for *E. huxleyi* [*Poulton et al*., 2010].
[c]Estimated from calcite production using cellular calcification to photosynthesis ratio of 0.7 [*Poulton et al*., 2010].
[d]Estimate of percentage of nonactive cells used to adjust PhytoC, Chl, and PP contributions.
[e]Estimated from cell counts using 0.35 pmol C cell^{-1} and 0.105 pg Chl cell^{-1} for *Fragilariopsis* (see text).
[f]Estimated from cell counts, cell carbon, and an estimate of community growth rate ($\mu = 1/\text{PhytoC} \times \text{PP}$).

associated with elevated Chl and POC (Table 2). No significant differences (one-way ANOVAs, $p > 0.2$) between hydrographic or bloom provinces in terms of integrated BSi concentrations were found (Figure 2g).

3.4. Primary Production and Calcite Production

[19] Integrated euphotic zone PP varied from 18.1 to 106.0 mmol C m^{-2} d^{-1} (Table 2), with high PP associated with elevated concentrations of Chl ($r = 0.84$, $p < 0.001$, $n = 25$; not shown) and POC ($r = 0.67$, $p < 0.001$, $n = 23$; not shown). No significant differences between hydrographic or bloom provinces were found in terms of integrated PP (Figure 2h), with stations in each province showing the full range of PP. In contrast, CP varied from 0.2 to 7.3 mmol C m^{-3} d^{-1} (Table 2), with high CP associated with elevated PIC concentrations ($r = 0.84$, $p < 0.001$, $n = 24$). Although no significant differences in CP were observed between hydrographic provinces, significant differences (one-way ANOVA, $p < 0.005$) did exist between bloom provinces (Figure 2i). Ratios of CP to PP (mol:mol) varied from <0.01 to 0.25 (Table 2), with values >0.1 mostly associated with the outer bloom and central bloom regions, although these areas also had values considerably less than this.

4. Discussion

4.1. Ecology of the 2008 Coccolithophore Bloom

[20] *Emiliania huxleyi* B/C numerically dominated the 2008 bloom along the Patagonian Shelf in terms of both coccospheres and detached coccoliths, while *E. huxleyi* type A was restricted to warmer waters at the northern end of the shelf and shelf waters [*Poulton et al*., 2011]. Unlike coccolithophore blooms in the North Atlantic, which may contain other species of coccolithophore (e.g., *C. pelagicus* [*Fernandez et al*., 1993; *Harlay et al*., 2010]), the 2008 Patagonian Shelf bloom was completely dominated by *E. huxleyi* [*Poulton et al*., 2011], as shown by the low diversity values for the outer bloom and central bloom (Table 2). However, the bloom also contained high cell numbers (0.2–2.0 × 0^3 cells mL^{-1}) of a small (<10 μm) diatom of the genus *Fragilariopsis* (*F. pseudonana*, Figure 1d). Such high cell abundances were at least equal to, or in some cases higher, than bloom cell abundances of *E. huxleyi* (e.g., Stations 047, 102, and 108).

[21] In order to assess the relative roles of these two species to biomass and organic production (PP) for the 2008 bloom, we used cell counts and conversion terms to estimate *E. huxleyi* and *Fragilariopsis* percentage contributions to total Chl, phytoplankton carbon (phytoC), and PP (Table 3). A discrepancy not found previously occurred at several stations, with cell-based Chl and carbon estimates twice as high as those from rate based ones. We attribute this to the presence of a high number (>50%) of dead or metabolically inactive cells, as observed by *Holligan et al*. [1993b], rather than extremely low (<0.2) cellular ratios of calcification to photosynthesis (published range 0.4–1 [*Paasche*, 2002]). For *Fragilariopsis*, cell carbon (0.35 pmol C cell^{-1}) was calculated from cell size SEM measurements (4 × 2.5 × 2 μm), following *Hinz et al.* [2012], while a carbon to Chl ratio of 40 was used to calculate cell Chl (0.105 pg Chl cell^{-1}). These factors were then combined with cell counts to estimate *Fragilariopsis* contributions to total Chl and phytoC. *Fragilariopsis* contributions to PP were determined from estimates of phytoplankton community growth rates (i.e., $\mu = 1/\text{phytoC} \times \text{PP}$) and *Fragilariopsis* biomass.

[22] Estimates of *E. huxleyi* and *Fragilariopsis* contributions to total Chl, phytoC, and PP were similar with ranges from <1 to ~40% for both biomass and PP contributions (Table 3). Although both *E. huxleyi* and *Fragilariopsis* contributions to Chl and phytoC biomass were ~10% in the central bloom, there was a notable difference in terms of

hydrographic provinces with *E. huxleyi* highest in ASW and SFC and *Fragilariopsis* highest in NFC (Table 3). Integrated Chl was highest in the outer bloom region (Figure 2d), where *E. huxleyi* and *Fragilariopsis* contributions were low (Table 3), and in this region other diatoms (e.g., *Chaetoceros*, *Thalassiosira*, and *Pseudonitzschia*) may have been more important contributors. The 2008 bloom, especially the central bloom region with highly detached coccoliths (Figure 2b), actually represented a complex mosaic where either *E. huxleyi* or *Fragilariopsis* (or other species) contributed a greater fraction to total Chl, phytoC, and PP. The distribution of empty coccolithophore cells showed highest contributions occurring in the central bloom, which included ASW, NFC, and SFC waters (Table 3).

[23] The 2008 *E. huxleyi* bloom occurred in cold (<8°C), macronutrient-rich waters of the ASW (Table 1), and to a lesser extent NFC and SFC waters [*Painter et al*., 2010; *Poulton et al*., 2011]. High concentrations of nitrate (>10 μmol NO_x kg^{-1}) and phosphate (>0.8 μmol PO_4 kg^{-1}) are common across the Southern Ocean, where iron concentrations are low and limit phytoplankton growth and PP [*Boyd et al*., 2007]. Thus, the Patagonian Shelf coccolithophore bloom may be linked to iron availability, with macronutrient-rich Southern Ocean water flowing north (via the ASW, NFC, and SFC) over shelf sediments which supply iron to the community [*Garcia et al*., 2008]. Such sedimentary iron inputs associated with shallow topography are common features of phytoplankton blooms in the high-nutrient low-chlorophyll (HNLC) Southern Ocean [*Boyd et al*., 2007].

[24] The genus *Fragilariopsis* (including *F. pseudonana*) is a common diatom group across the South Atlantic Ocean, from the Scotia Sea [*Hinz et al*., 2012] to the Patagonian Shelf [*Cefarelli et al*., 2010], and it clearly made a significant contribution to the 2008 coccolithophore bloom in terms of biomass and PP. Concentrations of dSi in the ASW, NFC, and SFC were also low (<2 μmol Si kg^{-1}; Table 1) and potentially limiting to diatom growth [e.g., *Egge and Aksnes*, 1992], conditions associated with a positive selective pressure for coccolithophores [*Holligan et al*., 1993a; *Townsend et al*., 1994]. High cell abundances of small *Fragilariopsis* may appear paradoxical in this context; however, combining cell numbers with an estimate of cell opal content (0.045 pmol Si $cell^{-1}$), assuming a cell carbon to BSi ratio of 0.13 [*Brzezinski*, 1985], and estimated growth rates for the total community ($\mu = 1/\text{phytoC} \times \text{PP}$), gives an approximate estimate of the dSi requirements for *Fragilariopsis* along the shelf. These estimates (data not shown) indicate that small *Fragilariopsis* would only account for a drawdown of ~10–20% of the dSi concentrations present, and despite its high abundance, its small cell size (~5 μm) and low cellular BSi quota allows for *Fragilariopsis* growth in waters with low dSi concentrations.

4.2. Biogeochemistry and Dynamics of the 2008 Coccolithophore Bloom

[25] Ratios of CP to PP in coccolithophore blooms rarely exceed 0.5 (0.4 in this study; <0.4–0.5 in *Poulton et al*. [2007]), implying that a significant fraction of PP is done by noncalcifying organisms. These may include naked/haploid *E. huxleyi* [*Holligan et al*., 1993b], other nanoflagellates [*Balch et al*., 1991], or, in the case of the Patagonian Shelf, diatoms. High contributions from such species potentially elevate the Chl and PP inventories along the Patagonian Shelf, with both Chl and PP relatively high in the outer bloom region compared with elsewhere along the shelf (Figure 2d and 2h). Integrated CP from the central bloom (0.4–7.3 mmol C m^{-2} d^{-1}) are in agreement with similar measurements from other oceanic or shelf sea coccolithophore blooms, although at the lower end of values (Table 4). In terms of integrated calcite concentrations, the Patagonian Shelf also had lower values (<80 mmol C m^{-2} d^{-1}) than most other blooms studied around the world (generally ~100–700 mmol C m^{-2}; Table 4).

[26] Such differences in bloom CP and calcite inventories could arise from studies sampling different stages of bloom development and decline. Some studies have used the ratio of detached coccoliths to cells as an index of bloom development [e.g., *Lessard et al*., 2005; *Harlay et al*., 2010], with early phase blooms characterized by low ratios (e.g., <25) and the ratio increasing with time (>50–100) as coccolith production exceeds cellular division. In the central bloom region in 2008, the median ratio of detached coccoliths to cells was 43 (Table 4). Satellite images of surface calcite for the Patagonian Shelf also indicate that the 2008 bloom was in decline during the time of in situ sampling [*Painter et al*., 2010]. Hence, differences in bloom stages do not appear to explain the differences in calcite concentrations between the 2008 bloom and similar studies globally. Rather, we suggest that the ~50% less coccolith calcite content for the B/C relative to the A morphotype of *E. huxleyi* (~0.015 versus 0.033–0.035 pmol C $coccolith^{-1}$, respectively [*Poulton et al*., 2010, 2011]) led to the lower calcite inventories.

[27] Another characteristic of the 2008 Patagonian Shelf bloom that was notably different from other blooms was the estimated turnover time (doubling time) of bloom calcite (Table 4). For the 2008 bloom, we estimated a turnover time of ~7 days, similar to estimates for blooms studied by *Marañón and González* [1997] and *Harlay et al*. [2011], but much shorter than for the blooms studied by *Fernandez et al*. [1993] and *Harlay et al*. [2010]. Bloom turnover is a function of CP (i.e., coccolithophore physiology), the amount of (detrital) calcite, and the loss terms of calcite from the water column. Short turnover times indicate active and rapid loss terms for such features, with advection, aggregation, sinking, and grazing all acting to remove calcite from the water column [*Holligan et al*., 1983, 1993a, 1993b; *Poulton et al*., 2006; *Balch et al*., 2009]. Longer turnover times (e.g., 1991 Iceland Basin, Table 4) potentially indicate fundamentally different dynamics in terms of bloom maintenance and formation.

[28] The role of local hydrographic conditions in bloom dynamics also needs consideration. The Patagonian Shelf is characterized by strong currents (>70 cm s^{-1} or >60 km d^{-1} [*Painter et al*., 2010]) with strong frontal features parallel to the shelf, where cold water is carried north along the shelf break [see *Painter et al*., 2010, Figure 2A]. The 2008 coccolithophore bloom formed within ASW [*Painter et al*., 2010] and waters of the NFC and SFC (see high detached coccoliths in Figure 2b), between strong frontal boundaries to the north of the Falkland Islands, and hence, material may have concentrated in this area. Conversely, such strong horizontal gradients can also be important in dispersing patches of high reflectance [*Holligan et al*., 1993a; *Balch et al*., 2009]. In contrast, the Iceland Basin is characterized by weak currents (<25 km d^{-1}) and meandering flows and eddies [*Holligan et al*., 1993b]. These fundamental differences between physical environments may also relate to

Table 4. Comparison of Bloom Dynamics for Central Bloom Waters of the Patagonian Shelf[a]

Region (date)	Integrated CP (mmol C m^{-2} d^{-1})	Integrated Calcite (mmol C m^{-2})	Detached Coccoliths ($\times 10^3$ mL^{-1})	Coccolith: Cell Ratio	Bloom Stage	Turnover[b] (d)	Source(s)
Iceland Basin (June 1991)	9.5 (2–7)	210 (142–277)	200 (100–300)	60 (12–108)	Late	~26	*Fernandez et al.* [1993]
North Sea (June 1996)	11.5	129.5	24–50	21 (7–34)	Early	~7	*Marañón and González* [1997]
Northern Bay of Biscay (June 2004)	6.4 (1.2–11.6)	199 (53–344)	27 (1–53)	7 (3–10)	Intermediate	~27	*Harlay et al.* [2010]
Northern Bay of Biscay (June 2006)	30 (7.5–51.7)	435 (200–670)	-	-	Intermediate	~10	*Harlay et al.* [2011]
Patagonian Shelf, (December 2008)	4 (0.4–7.3)	43 (6–80)	26 (12–40)	43 (13–3)	Late[b]	~7	[b]*Painter et al.* [2010, *this study*]

[a]Medians are given, with ranges in brackets.
[b]Turnover times calculated as natural log $2/\mu$, where μ was calculated as $\mu = 1/\mathrm{PIC} \times \mathrm{CP}$ in this case.

differences in bloom dynamics and may be applicable globally to blooms in different locations.

[29] Coccolithophore blooms occur at multiple scales, from large (>250,000 km^2) oceanic features, such as in the Iceland Basin and western North Atlantic [*Holligan et al.*, 1993b; *Brown and Yoder*, 1994], to smaller scale features (<100,000 km^2) associated with continental shelves [*Balch et al.*, 1991; *Holligan et al.*, 1983, 1993a, this study]. When calcite concentrations are scaled to the areal extent of these blooms, strong differences can be seen with the 1991 Iceland Basin bloom representing ~1 MtC [*Holligan et al.*, 1993b], while the 2008 Patagonian Shelf bloom produced ~50 times less (~0.02 MtC) despite only being ~ half the size (~66,000 km^2 [*Painter et al.*, 2010]). Central to this difference is the ~5–10 times lower calcite concentrations found in the 2008 bloom (Table 4), which we suggest are due to the dominance of the B/C morphotype of *E. huxleyi*.

4.3. Physiology of *Emiliania huxleyi* in the 2008 Bloom

[30] Elucidating variability in coccolithophore physiology, and the factors influencing coccolithophore calcification, requires more than just simple comparisons of cell numbers (or CP) with environmental factors, as both growth and mortality control population densities (and CP), and there is considerable cellular variability in the rate of calcification with growth conditions [*Paasche*, 2002; *Poulton et al.*, 2010]. An alternative approach is to consider cellular levels of calcification in the form of cell-normalized rates (cell-CF), which are proportional to coccolith production rates when normalized to coccolith calcite content and the community consists of one or a few species [*Poulton et al.*, 2010]. Under nutrient replete culture conditions, *E. huxleyi* can produce coccoliths at a rate of one every 20–40 min (1.5 to 3 coccoliths $cell^{-1}$ h^{-1}) and attain cell-CF rates of ~0.2–0.8 pmol C $cell^{-1}$ d^{-1} [*Paasche*, 1962; *Balch et al.*, 1996b]. A field study of nonbloom *E. huxleyi* (morphotype A) dominated populations in the Iceland Basin by *Poulton et al.* [2010] found similar cell-CF (0.25–0.75 pmol C $cell^{-1}$ d^{-1}) to culture studies, which were equivalent to coccolith production rates of 0.4 to 1.8 coccoliths $cell^{-1}$ h^{-1}, using a coccolith calcite content of 0.033 pmol C.

[31] Using the revised cell counts (see section 4.1, Figure 3a) we estimate cell-CF for the coccolithophore populations along the Patagonian Shelf of between 0.07 and 0.65 pmol C $cell^{-1}$ d^{-1} (Figure 3b), with a cruise average (± standard deviation) of 0.35 (± 0.17) pmol C $cell^{-1}$ d^{-1}. These values are similar to values for the nonbloom community in the Iceland Basin [*Poulton et al.*, 2010], and there is little obvious trend or difference between the different hydrographic or bloom provinces along the Patagonian Shelf (Figure 3b, one-way ANOVA, $p > 0.5$). When normalized to estimated coccolith calcite content [*Poulton et al.*, 2011], coccolith production rates also range over the full physiological spectrum (0.3 to 3.3 coccoliths $cell^{-1}$ h^{-1}; Figure 3c), slightly higher than in the Iceland Basin. A lack of significant differences in coccolith production rates between the non-bloom and central bloom regions (one-way ANOVA, $p > 0.6$) indicate that the 2008 bloom was maintained by high cell numbers. If 12–15 coccoliths are necessary to form a new coccosphere [*Balch et al.*, 1996] then the community along the shelf was producing ~2–3 times this number per (15 h) day, which indicates excessive coccolith production in bloom waters.

[32] The 2008 bloom occurred in waters with slightly lower Ω_C (<3.5) than to the north of the shelf (Table 1) [*Poulton et al*., 2011]. The dominant B/C morphotype of *E. huxleyi* has a lower calcite content than the A morphotype [*Cook et al*., 2011; *Poulton et al*., 2011], which appeared restricted to low-nutrient, warmer (>8°C) waters to the north of the shelf, with higher Ω_C. Recent studies have linked reduced coccolithophore calcification rates (using coccolith calcite as a proxy) with lower Ω_C [e.g., *Cubillos et al*., 2007; *Beaufort et al*., 2011], and our data are generally supportive of this trend. However, coccolith production rates, based on the combination of cell-CF and coccolith calcite content, are physiologically high (up to three per hour) in bloom waters with lower saturation states. Clearly, cellular calcification is a product of not just the calcite content of individual coccoliths but also the rate of their production. Formation of a new coccosphere, by cells during division, is clearly a physiological driver for their production [*Balch et al*., 1996b], and hence, we suggest that coccolith production is a better measure of coccolithophore physiology than the amount of calcite in each coccolith (i.e., the degree of calcification per coccolith).

5. Conclusions

[33] Relative to many other coccolithophore blooms in the global ocean, the 2008 Patagonian Shelf bloom was uniquely dominated by the B/C morphotype of *E. huxleyi* [*Poulton et al*., 2011] and had high abundances of small (<10 μm) *Fragilariopsis* diatoms (likely *F. pseudonana*), and these two made almost equal contributions to total Chl, phytoC, and PP (Table 3). Hence, our observations highlight how coccolithophore blooms differ globally and represent complex mosaics of inorganic and organic production. Both *Cook et al*. [2011] and *Poulton et al*. [2011] have suggested that *E. huxleyi* type B/C is a Southern Ocean specialist and may dominate communities in the Scotia Sea [*Hinz et al*., 2012]. Small *Fragilariopsis* are also common throughout the Scotia and Weddell Seas [*Cefarelli et al*., 2010; *Hinz et al*., 2012], and it appears that the 2008 coccolithophore bloom, which occurred in cold, macronutrient-rich water, was also dominated by a flora more representative of the Southern Ocean. High residual macronutrient concentrations (i.e., HNLC conditions) at the southern end of the shelf (Table 1) also support a Southern Ocean link and imply a potential role for micronutrient availability in bloom dynamics [*Garcia et al*., 2008].

[34] Indices of the degree of cellular calcification, including coccolith calcite content [*Poulton et al*., 2011], cell-specific calcification, and individual coccolith production rates (Figures 3b and 3c), indicate that the shelf community was producing coccoliths at physiologically high rates, in excess of the number needed to make a new coccosphere daily. When sampled, the 2008 coccolithophore bloom was in decline [*Painter et al*., 2010], despite high cellular rates of calcification, and therefore, we conclude that the relatively low inventories of calcite present in bloom waters were due to dominance of the low-calcite B/C morphotype.

[35] High reflectance signals, indicative of coccolithophore blooms, are common features in the Southern Ocean (e.g., South Georgia, Polar Frontal Zone) [*Holligan et al*., 2010]. The dominance of *E. huxleyi* type B/C in many parts of the Southern Ocean [e.g., *Cubollis et al*., 2007; *Cook et al*., 2011; *Poulton et al*., 2011; *Hinz et al*., 2012] implies that this morphotype dominates high-reflectance features in the Southern Hemisphere and these may be characterized by low areal calcite content relative to similar sized features in the Northern Hemisphere which may be dominated by type A. Importantly, our observations from the Patagonian Shelf indicate that bloom morphotype composition has a global significance in terms of coccolithophore bloom dynamics, specifically the magnitude of calcite production and export of these features.

[36] Establishing that *E. huxleyi* morphotype variability has a direct impact on the calcite yield of coccolithophores, including blooms, signifies that understanding global morphotype biogeography [e.g., *Cubillos et al*., 2007] and comparative physiology [e.g., *Cook et al*., 2011] are key steps in understanding global calcite production. When viewed in the context of climate change, our observations indicate that biogeographical shifts in the morphotypes of *E. huxleyi* [e.g., *Cubillos et al*., 2007] will influence oceanic calcite production. Furthermore, strain-specific variability in the sensitivity of *E. huxleyi* to ocean acidification [*Langer et al*., 2009, 2011], potentially linked to morphotype variability, could ultimately have important implications for the marine carbon cycle. For example, if morphotypes with lower (or higher) coccolith calcite content are favored by higher pCO_2 conditions, then global coccolithophore calcite production may decrease (or increase).

[37] **Acknowledgments.** A.J.P. and S.C.P. were supported by the Natural Environmental Research Council (Oceans 2025 funding, NE/F015054/1 and NE/H017097/1). W.M.B. was supported by National Science Foundation (OCE-0728582 and OCE-0961660) and National Aeronautics and Space Administration (NNX08AJ88A and NNX08AAB10G). We thank Dan Schuller (SCRIPPS) for macronutrient measurements; John Allen, Rosland Pidcock, Charlotte Marcinko, and Stephanie Henson (NOC) for assistance with physical and satellite PAR data; and Marlene Jeffries, Keven Neely, Rebecca Garley (BIOS), and Nicole Beniot (WHOI) for assistance with seawater carbonate chemistry. MODIS Aqua data were obtained from the NASA Ocean Color distributed archive (http://oceancolor.gsfc.nasa.gov/).

References

Balch, W. M., P. M. Holligan, S. G. Ackleson, and K. J. Voss (1991), Biological and optical properties of mesoscale coccolithophore blooms in the Gulf of Maine, *Limnol. Oceanogr.*, *36*(4), 629–643.

Balch, W. M., K. A. Kilpatrick, P. Holligan, D. Harbour, and E. Fernandez (1996a), The 1991 coccolithophore bloom in the central North Atlantic. 2. Relating optics to coccolith concentration, *Limnol. Oceanogr.*, *41*(8), 1684–1696.

Balch, W. M., J. J. Fritz, and E. Fernández (1996b), Decoupling of calcification and photosynthesis in the coccolithophore *Emiliania huxleyi* under steady-state light-limited growth, *Mar. Ecol. Prog. Ser.*, *142*, 87–97.

Balch, W. M., D. Drapeau, and J. Fritz (2000), Monsoonal forcing of calcification in the Arabian Sea, *Deep Sea Res. Part II*, *47*, 1301–1337.

Balch, W. M., A. J. Plueddeman, B. C. Bowler, and D. T. Drapeau (2009), Chalk-Ex—Fate of CaCO3 particles in the mixed layer: Evolution of patch optical properties, *J. Geophys. Res.*, *114*, C07020, doi:10.1029/2008JC004902.

Balch, W. M., A. J. Poulton, D. T. Drapeau, B. C. Bowler, L. A. Windecker, and E. S. Booth (2011), Zonal and meridional patterns of phytoplankton biomass and carbon fixation in the Equatorial Pacific Ocean, between 110°W and 140°W, *Deep Sea Res. Part II*, *58*, 400–416, doi:10.1016/j.dsr2.2010.08.004.

Bates, N. R., A. F. Michaels, and A. H. Knap (1996), Seasonal and interannual variability of oceanic carbon dioxide species at US JGOFS Bermuda Atlantic Time-series Study (BATS) site, *Deep Sea Res. Part II*, *43*, 347–383.

Beaufort, L., et al. (2011), Sensitivity of coccolithophores to carbonate chemistry and ocean acidification, *Nature*, *476*, 80–83, doi:10.1038/nature10295.

Bianchi, A. A., D. R. Pino, H. G. I. Perlender, A. P. Osiroff, V. Segura, V. Lutz, M. L. Clara, C. F. Balestrini, and A. R. Piola (2009), Annual balance and seasonal variability of sea-air CO2 fluxes in the Patagonian Sea: Their relationship with fronts and chlorophyll distribution, *J. Geophys. Res.*, *114*, C03018, doi:10.1029/2008JC004854.

Boyd, P. W., et al. (2007), Mesoscale iron enrichment experiments 1993–2005: Synthesis and future directions, *Science*, *315*, 612–615, doi:10.1126/science.1131669.

Brown, C. W., and G. P. Podesta (1997), Remote sensing of coccolithophore blooms in the western South Atlantic Ocean, *Remote Sens. Environ.*, *60*, 83–91.

Brown, C. W., and J. A. Yoder (1994), Coccolithophorid blooms in the global ocean, *J. Geophys. Res.*, *99*, 7467–7482.

Brzezinski, M. (1985), The Si:C:N ratio of marine diatoms: Interspecific variability and the effect of some environmental variables, *J. Phycol.*, *21*, 347–357.

Brzezinski, M., and D. M. Nelson (1989), Seasonal changes in the silicon cycle within a Gulf Stream warm-core ring, *Deep Sea Res. Part I*, *36*, 1009–1030.

Cefarelli, A. O., M. E. Ferrario, G. O. Almandoz, A. G. Atencio, R. Akselman, and M. Vernet (2010), Diversity of the diatom genus *Fragilariopsis* in the Argentine Sea and Antarctic waters: Morphology, distribution and abundance, *Polar Biol.*, *33*, 1463–1484, doi:10.1007/s00300-010-0794-z.

Cook, S. S., L. Whittock, S. W. Wright, and G. M. Hallegraeff (2011), Photosynthetic pigment and genetic differences between two southern Ocean morphotypes of *Emiliania huxleyi* (Haptophyta), *J. Phycol.*, *47*, 615–626, doi:10.1111/j.1529-8817.2011.00992.x.

Cubillos, J. C., S. W. Wright, G. Nash, M. F. de Salas, B. Griffiths, B. Tilbrook, A. Poisson, and G. M. Hallegraeff (2007), Calcification morphotypes of the coccolithophorid *Emiliania huxleyi* in the Southern Ocean: Changes in 2001to 2006 compared to historical data, *Mar. Ecol. Prog. Ser.*, *348*, 47–54, doi:10.3354/meps07058.

Dickson, A. G., and F. J. Millero (1987), A comparison of the equilibrium constants for the dissociation of carbonic acid in seawater media, *Deep Sea Res. Part A*, *34*, 1733–1743.

Dickson, A. G., C. L. Sabine, and J. R. Christian (2007) Guide to best practices for ocean CO2 measurements. PICES Special Publication Vol. 3, IOCCP report no. 8.

Egge, J. K., and D. L. Aksnes (1992), Silicate as regulating nutrient in phytoplankton competition, *Mar. Ecol. Prog. Ser.*, *83*, 281–289.

Fernandez, E., P. Boyd, P. M. Holligan, and D. S. Harbour (1993), Production of organic and inorganic carbon within a large-scale coccolithophore bloom in the northeast Atlantic Ocean, *Mar. Ecol. Prog. Ser.*, *97*, 271–285.

Frada, M., J. R. Young, M. Cachão, S. Lino, A. Martins, A. Narciso, I. Probert, and C. De Vargas (2010), A guide to extant coccolithophores (Calcihaptophycidae, Haptophyta) using light microscopy, *J. Nannoplankton Res.*, *31*(2), 58–112.

Fritz, J. J. (1999), Carbon fixation and coccolith detachment in the coccolithophore *Emiliania huxleyi* in nitrate-limited cyclostats, *Mar. Biol.*, *133*, 509–518.

Fritz, J. J., and W. M. Balch (1996), A light-limited continuous culture study of *Emiliania huxleyi*: Determination of coccolith detachment and its relevance to cell sinking, *J. Exp. Mar. Biol. Ecol.*, *207*, 127–147.

Garcia, V. M. T., C. A. E. Garcia, M. M. Mata, R. C. Pollery, A. R. Piola, S. R. Signorini, C. R. McClain, and M. D. Iglesias-Rodriguez (2008), Environmental factors controlling the phytoplankton blooms at the Patagonian Shelf-break in spring, *Deep Sea Res. Part I*, *55*, 1150–1166, doi:10.1016/j.dsr.2008.04.011.

Garcia, C. A. E., V. M. T. Garcia, A. I. Dogliotti, A. Ferreira, S. I. Romero, A. Mannino, M. S. Souza, and M. M. Mata (2011), Environmental conditions and bio-optical signature of a coccolithophorid bloom in the Patagonian Shelf, *J. Geophys. Res.*, *116*, C03025, doi:10.1029/2010JC006595.

Grasshoff, K., M. Ehrhardt, and K. Kremling (1983), *Methods of Seawater Analysis*, Verlag Chemie, Weinheim.

Harlay, J., et al. (2010), Biogeochemical study of a coccolithophore bloom in the northern Bay of Biscay (NE Atlantic Ocean) in June 2004, *Prog. Oceanogr.*, *86*, 317–336, doi:10.1016/j.pocean.2010.04.029.

Harlay, J., et al. (2011), Biogeochemistry and carbon mass balance of a coccolithophore bloom in the northern Bay of Biscay (June 2006), *Deep Sea Res. Part I*, *58*, 111–127, doi:10.1016/j.dsr.2010.11.005.

Haxo, F. T. (1985), Photosynthetic action spectrum of the coccolithophorid *Emiliania huxleyi* (Haptophyceae): 19'-Hexanoyloxyfucoxanthin as antenna pigment, *J. Phycol.*, *21*, 282–287.

Hinz, D. J., A. J. Poulton, M. C. Nielsdóttir, S. Steigenberger, R. E. Korb, E. P. Achterberg, and T. S. Bibby (2012), Comparative seasonal biogeography of mineralising nannoplankton in the Scotia Sea: *Emiliania huxleyi*, *Fragilariopsis* spp. and *Tetraparma pelagica*, *Deep Sea Res. Part II*, *59-60*, 57–66, doi:10.1016/j.dsr2.2011.09.002.

Holligan, P. M., M. Viollier, D. S. Harbour, P. Camus, and M. Champagne-Philippe (1983), Satellite and ship studies of coccolithophore production along a continental shelf edge, *Nature*, *304*, 339–342.

Holligan, P. M., et al. (1993a), A biogeochemical study of the coccolithophore, *Emiliania huxleyi*, in the North Atlantic, *Global Biogeochem. Cycles*, *7*, 879–900.

Holligan, P. M., S. B. Groom, and D. S. Harbour (1993b), What controls the distribution of the coccolithophore, *Emiliania huxleyi*, in the North Sea?, *Fish. Oceanogr.*, *2*, 175–183.

Holligan, P. M., A. Charalampopoulou, and R. Hutson (2010), Seasonal distributions of the coccolithophore, *Emiliania huxleyi*, and of particulate inorganic carbon in surface waters of the Scotia Sea, *J. Mar. Syst.*, *82*, 195–205, doi:10.1016/j.marsys.2010.05.007.

Iglesias-Rodriguez, M. D., C. W. Brown, S. C. Doney, J. Kleypas, D. Kolber, Z. Kolber, P. K. Hayes, and P. G. Falkowski (2002), Representing key phytoplankton functional groups in ocean carbon models: Coccolithophorids, *Global Biogeochem. Cycles*, *16*(4), 1100, doi:10.1029/2001GB001454.

Joint Global Ocean Flux Study (JGOFS) (1996), a, 170 pp. Scientific Committee on Oceanic Research, International Council of Scientific Unions, Intergovernmental Oceanographic Commission.

Langer, G., G. Nehrke, I. Probert, J. Ly, and P. Ziveri (2009), Strain-specific responses of *Emiliania huxleyi* to changing seawater carbonate chemistry, *Biogeosciences*, *6*, 2637–2646.

Langer, G., I. Probert, G. Nehrke, and P. Ziveri (2011), The morphological response of *Emiliania huxleyi* to seawater carbonate chemistry changes: An inter-strain comparison, *J. Nannoplankton Res.*, *32*(1), 29–34.

Lessard, E. J., A. Merico, and T. Tyrrell (2005), Nitrate:phosphate ratios and *Emiliania huxleyi*, *Limnol. Oceanogr.*, *50*(3), 1020–1024.

Marañón, E., and N. González (1997), Primary production, calcification and macromolecular synthesis in a bloom of the coccolithophore *Emiliania huxleyi* in the North Sea, *Mar. Ecol. Prog. Ser.*, *157*, 61–77.

Mehrbach, C., C. H. Cuberson, J. E. Hawley, and R. M. Pytkowicz (1973), Measurement of the apparent dissociation constants of carbonic acid in seawater at atmospheric pressure, *Limnol. Oceanogr.*, *18*, 897–907.

Müller, M. N., A. N. Antia, and J. LaRoche (2008), Influence of cell cycle phase on calcification in the coccolithophore *Emiliania huxleyi*, *Limnol. Oceanogr.*, *53*(2), 506–512.

Paasche, E. (1962), Coccolith formation, *Nature*, *193*, 1094–1095.

Paasche, E. (2002), A review of the coccolithophorid *Emiliania huxleyi* (Prymnesiophyceae), with particular references to growth, coccolith formation, and calcification-photosynthesis interactions, *Phycologia*, *40*, 5003–5029.

Paasche, E., and S. Brubak (1994), Enhanced calcification in the coccolithophorid *Emiliania huxleyi* (Haptophyceae) under phosphorus limitation, *Phycologia*, *33*(5), 324–330.

Painter, S. C., A. J. Poulton, J. T. Allen, R. Pidcock, and W. M. Balch (2010), The COPAS'08 expedition to the Patagonian Shelf: Physical and environmental conditions during the 2008 coccolithophore bloom, *Cont. Shelf Res.*, *30*, 1907–1923, doi:10.1016/j.csr.2010.08.013.

Pierrot, D. E., E. Lewis, and D. W. R. Wallace (2006), *MS Excel Program Developed for CO_2 System Calculations*, ORNL/CDIAC-105a, Carbon Dioxide Information Analysis Centre, Oak Ridge National Laboratory, US Department of Energy, Oak Ridge, Tenn.

Poulton, A. J., R. Sanders, P. M. Holligan, M. C. Stinchcombe, T. R. Adey, L. Brown, and K. Chamberlain (2006), Phytoplankton mineralization in the tropical and subtropical Atlantic Ocean, *Global Biogeochem. Cycles*, *20*, GB4002, doi:10.1029/2006GB002712.

Poulton, A. J., T. R. Adey, W. M. Balch, and P. M. Holligan (2007), Relating coccolithophore calcification rates to phytoplankton community dynamics: Regional differences and implications for carbon export, *Deep Sea Res. Part II*, *54*, 538–557, doi:10.1016/j.dsr2.2006.12.003.

Poulton, A. J., A. Charalampopoulou, J. R. Young, G. A. Tarran, M. I. Lucas, and G. D. Quartly (2010), Coccolithophore dynamics in non-bloom conditions during late summer in the central Iceland Basin (July–August 2007), *Limnol. Oceanogr.*, *55*(4), 1601–1613, doi:10.4319/lo.2010.55.4.1601.

Poulton, A. J., J. R. Young, N. R. Bates, and W. M. Balch (2011), Biometry of detached *Emiliania huxleyi* coccoliths along the Patagonian Shelf, *Mar. Ecol. Prog. Ser.*, *443*, 1–17, doi:10.3354/meps09445.

Schloss, I. R., G. A. Ferreyra, M. E. Ferrario, G. O. Almandoz, R. Codna, A. A. Bianchi, C. F. Balestrini, H. A. Ochoa, D. R. Pino, and A. Poisson (2007), Role of plankton communities in sea-air variations in pCO_2 in the SW Atlantic Ocean, *Mar. Ecol. Prog. Ser.*, *332*, 93–106.

Scott, F. J., and H. J. Marchant (2005), *Antarctic Marine Protists*, Australian Biological Resources Study, Canberra, Australia.

Signorini, S. R., V. M. T. Garcia, A. R. Piola, C. A. E. Garcia, M. M. Mata, and C. R. McClain (2006), Seasonal and inter-annual variability of calcite in the vicinity of the Patagonian Shelf break (38°S–52°S), *Geophys. Res. Lett.*, *33*, L16610, doi:10.1029/2006GL026592.

Townsend, D. W., M. D. Keller, P. M. Holligan, S. G. Ackleson, and W. M. Balch (1994), Blooms of the coccolithophore *Emiliania huxleyi* with respect to hydrography in the Gulf of Maine, *Cont. Shelf Res.*, *14*, 979–1000.

Tyrrell, T., and A. Merico (2004), *Emiliania huxleyi*: Bloom observations and the conditions that induce them, in *Coccolithophores: From Molecular Processes to Global Impact*, edited by H. R. Thierstein and J. R. Young, pp. 75–97, Springer-Verlag, Heidelberg.

Young, J. R., M. Geisen, L. Cros, A. Kleijne, C. Sprengel, I. Probert, and J. B. Østergaard (2003), A guide to extant calcareous nannoplankton taxonomy, *J. Nannoplankton Res. Spec. Iss.*, *1*, 1–125.